Eng. Sci., 2021, **13**, 71–78

Engineered Science

DOI: https://dx.doi.org/10.30919/es8d1263

Composite of Strip-shaped ZIF-67 with Polypyrrole: A Conductive Polymer-MOF Electrode System for Stable and High Specific Capacitance

Sajid ur Rehman,[1] Rida Ahmed,[2] Kun Ma,[1] Shuai Xu,[1] Tongxiang Tao,[1] Muhammad Adnan Aslam,[1] Muhammad Amir[3] and Junfeng Wang[1, 4,*]

Abstract

Strips like Zeolitic imidazolate framework-67 (SZIF-67) have been prepared by the wet chemical method and polypyrrole (PPy) has been deposited on the surface through the in-situ polymerization method and named as SZIF-67@PPy. The structure and morphology of prepared samples were observed by Scanning electron microscope (SEM), Transmission electron microscope (TEM), X-ray diffraction (XRD) and X-ray Photoelectron Spectroscopy (XPS). Further, the prepared samples (PPY, SZIF-67 and SZIF-67@PPy) were used as active electrode materials of supercapacitors. Compared with PPy and SZIF-67, the results show that SZIF-67@PPy has enhanced electrochemical performance, high-rate capability and good cycle stability. The results indicate that SZIF-67@PPy can become the next generation electrode materials for high-performance flexible supercapacitors.

Keywords: ZIF-67; Polypyrrole; Polymerization; Electrode.
Received: 24 November 2020; Accepted: 13 December 2020.
Article type: Research article.

1. Introduction

In recent years, supercapacitors have attracted more and more attention. Because of their small size, high flexibility and wearability, they have a broad future in the next generation of wearable electronic devices. In general, supercapacitors can be divided into two types: one is EDLCs and the other is pseudocapacitors.[1,2] In general, EDLCs capacitors are mainly made of carbon-based materials, especially graphite and graphene oxide (GO), which are usually preferred because of their good conductivity, high specific surface area and long-term stability.[3,4] However, the specific capacitance of the bilayer capacitor is not likely to be too high due to the storage mechanism of charge.[5,6] On the contrary, the specific capacitance of the pseudocapacitor is 10-100 times higher than EDLCs capacitors. Because of the Faradic charge storage mechanism, the specific capacitance is mainly the redox reaction of the active electrode material.[7,8]

Conductive polymers (CPs, such as polypyrrole (PPy) and polyaniline (PANI)), metal oxides and metal halides are commonly used as active materials for pseudocapacitors, among which CPs are more promising for flexible supercapacitors. In recent years, due to the advantages of polypyrrole (such as high conductivity, simple preparation, low price, high energy density, and good cycle stability), it is widely used in the production of supercapacitor electrode materials. Although research on PPy composite supercapacitor has developed rapidly in recent years, there are still some problems to be overcome in the process of device production, such as the simultaneous improvement of the power density and energy density as well as the development of an environment-friendly electrolyte system, and intelligent wearable devices.[9,10] In the electrode materials of hybrid supercapacitors, the electrochemical charge storage capacity of the pseudocapacitor results from the charge separation of electrons and ions at the electrode-electrolyte interface.[11] On the other hand, the induce charge transfer mechanism makes the charge storage capacity at the interface of the electrode-electrolyte significantly enhanced. However, the realization of high specific capacitance depends on many factors, such as the

[1] *CAS Key Laboratory of High Magnetic Field and Ion Beam Physical Biology, Hefei Institutes of Physical Science, Chinese Academy of Sciences, Hefei, Anhui, 230031, China.*
[2] *School of Physics & Material Science, Anhui University, Hefei, 230601, China.*
[3] *Key Laboratory of Materials Modification by Laser, Ion and Electron Beams, Chinese Ministry of Education, School of Physics, Dalian University of Technology, Dalian, 116024, China.*
[4] *Institutes of Physical Science and Information Technology, Anhui University, Hefei, 230601, China.*
* E-mail: junfeng@hmfl.ac.cn (J. Feng)

effective surface area of the active material, the rate of ion transport and migration, and more importantly, the adsorbed ion concentration and the induced charge transfer efficiency in the pseudocapacitance plays an important role.[12]

PPy is a kind of common conductive polymer material, which was found earlier and studied thoroughly at present.[13] Its application and mechanism are still the research hotspot in recent years.[14,15] As early as 1963, Weiss *et al*. report some examples of highly conductive PPy through the pyrolysis of tetraiodapyrrole.[16] In 2000, MacDiarmid received the Nobel prize on explaining the "benzene structure" and metallic conductivity in organic polymers.[17] With the development of polypyrrole performance research, the research direction has gradually shifted from single electrical performance to magnetic, electromagnetics and other fields.[18–22] Zeolitic imidazolate framework-67 (ZIF-67) is a special class of MOFs contained imidazolate linkers through coordination, supramolecular and hydrogen bonding interactions contains porous network and a periodic structure.[23–26] ZIF-67 is a good option for the supercapacitor electrode because of the porous structure providing fast ion diffusion and rich interfacial active sites that can speed up faradaic reactions.[27,28] However, as prepared ZIF-67 have typically poor electrical conductivity that limits their utilization for electrochemical applications. The constraint of poor electrical conductivity of ZIF-67 can be fixed through the composite of conducting polymer such as PPy with ZIF-67.

In this paper, strip-shaped ZIF-67 (SZIF-67) has been prepared by the wet chemical method and PPy has been deposited on the surface by the in-situ polymerization method and named as SZIF-67@PPy. Subsequently, the SZIF-67@PPy has been used as active electrode materials of supercapacitors. The results show that SZIF-67@PPy has decent electrochemical performance, high rate performance and good cycle stability compared with PPy and ZIF-67. The encouraging results make SZIF-67@PPy a promising electrode material for high-performance flexible supercapacitors.

2. Experimental

2.1 Reagent Used

Pyrrole (analytical pure, redistilled before use, from Shanghai Zhenxing chemical); persulfate amine, (APS, analytical pure, directly used after the purchase, from Sinopharm Group Co., Ltd.); camphor sulfonic acid, (CSA, analytical pure, directly used after the purchase, from Sinopharm Group Co., Ltd.); 2-methylimidazole (98% analytical pure, directly used after purchase, Aladin corporation); Cobalt nitrate hexahydrate ($Co(NO_3)_2.6H_2O$; 99% analytical pure, directly used after purchase, Aladin corporation) and methanol (CH_3OH; 99.5% analytical pure, directly used after purchase, Sinopharm chemical reagent co.). The deionized water was used throughout the experiment.

2.2 Preparation of SZIF-67

Homogenous 0.25 M solution of $Co(NO_3)_2.6H_2O$ (named as sol. A) and 1 M of $C_4H_6N_2$ (named as a sol. B) in methanol are prepared. Then, the sol. A is added quickly into sol. B with slow stirring. The resulted purple-colored solution is left undisturbed at room temperature for 10 days. The precipitates from the solution were collected by centrifuge and washed with deionized water, the obtained precipitate was dried at 40 °C overnight to obtain SZIF-67.

2.3 Preparation of SZIF-67@PPy

0.805 g of pyrrole monomer, 0.4 g CSA and an appropriate amount of SZIF-67 (1 g) were added into 500 ml deionized water under magnetic stirring. 2.73 g of APS was dissolved into 500 ml deionized water separately. The molar ratio of ammonium persulfate and pyrrole monomer was 1:1. The APS solution was added dropwise into the pyrrole containing solution at a constant speed, stir it quickly, and leave the mixed solution to react at room temperature for 20 hours. After the reaction, the samples were washed with DI water/ethanol and then dried in a vacuum for 24 hours at 40 ˚C to obtain SZIF-67@PPy.

2.4 Testing and characterization

Scanning electron microscope (SEM): The solid powder samples were ultrasonically dispersed in anhydrous ethanol, and then the mixed liquid was dropped on the clean silicon wafer. The micromorphology of the samples was observed by the s-4800 field emission electron microscope (Hitachi, Japan). Transmission electron microscope (TEM): The solid powder samples were dispersed by ultrasonic in anhydrous ethanol, uniformly dispersed and dropped on the copper substrate, and then the microstructure of the samples was characterized by JEM-2100 high-resolution transmission electron microscope (Hitachi, Japan).

X-ray diffraction (XRD) and X-ray Photoelectron Spectroscopy (XPS): The X-ray diffraction analyzer was carried out by XD-3 (Beijing Universal Instruments Co., Ltd). The scanning speed is 4°/min, λ = 0.15405 nm, the scanning angle (2θ) range is between 5° - 80°. X-ray Photoelectron Spectroscopy (XPS) was carried out by ESCALAB 250. Electron paramagnetic resonance (EPR) spectroscopy: Samples were tested for EPR on Bruker EMX plus 10/12 (equipped with Oxford ESR910 Liquid Helium cryostat) at room temperature (298 K). Brunauer–Emmett–Teller (BET) surface area: The BET surface area of the samples (SZIF-67, PPy and SZIF-67@PPy) were measured on a Micromeritics ASAP 2020 analyzer by N_2 adsorption at -196 °C.

Electrochemical test: The electrochemical performance was tested by chi-660e electrochemical workstation, and cyclic voltammetry (CV), constant current charge-discharge (GCD) and electrochemical impedance spectroscopy (EIS) were tested by a traditional three-electrode system. Platinum electrode and saturated calomel electrode (SCE) were used as counter electrode and reference electrode, respectively. The potential window of CV and GCD is -0.4 - 0.6 V (vs.SCE). The working electrode is composed of 80% as-synthesized composite material, 10% conductive carbon (acetylene black)

and 10% binder (polytetrafluoroethylene: PTFE). The above mixture is coated onto a piece of carbon cloth (1 × 1 cm^2) with a loading of ~5.0 mg cm^{-2} and then vacuum dried for 12 hours at 45 °C. The electrolyte is 1 M H_2SO_4 aqueous solution.

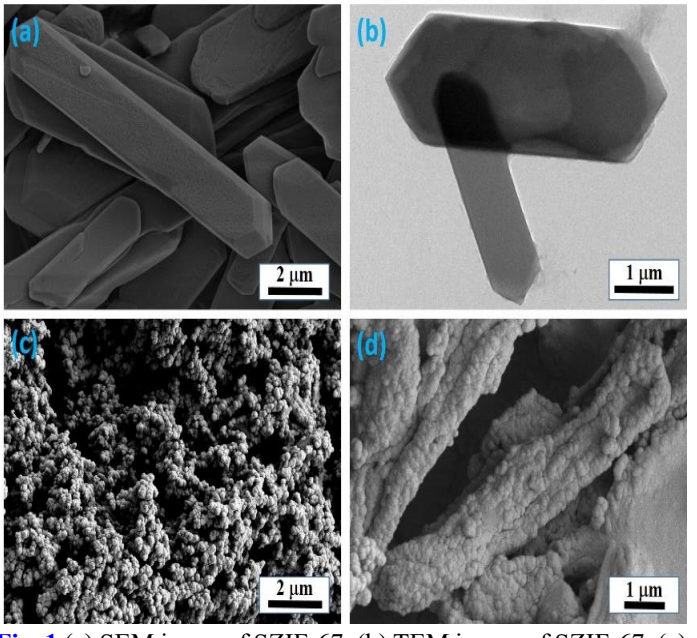

Fig. 1 (a) SEM imageof SZIF-67, (b) TEM image of SZIF-67, (c) SEM image of PPy and (d) SEM image of SZIF-67@PPy composite, respectively.

3. Results and discussion

Fig. 1 shows the SEM images of SZIF-67 (a), PPy (c) and SZIF-67@PPy (d), respectively. As shown in Fig. 1(a,b), the prepared SZIF-67 shows strips like structure which is different from the conventional rhombic dodecahedral shape of ordinary ZIF-67. It is due to the long reaction time at comparatively lower synthesis temperature (room temp.) and higher linker concentration, which provides sufficient time to the 2-MIM linker to form its structure. The average length and width of SZIF-67 are about 10 μm and 1.5 μm, respectively (illustrated in Fig. 1b). Fig. 1(c) illustrates the formation of PPy, which mainly presents a coral-like structure formed by uniform spheres and self-assembly. Fig. 1(d) shows the SEM images of the SZIF-67@PPy composite. Intriguingly, the surface of the composite of SZIF-67@PPy becomes rough compared with the SZIF-67. The small bumps on the surface of the composite directly related to the concentration of pyrrole monomers during the synthesis process. The surface of SZIF-67 is rich in organic groups so that it has a high affinity for the conjugated chains of PPy.

Fig. 2(a) shows the XRD pattern of SZIF-67, PPy and SZIF-67@PPy. The XRD pattern reveals the high crystalline nature of SZIF-67 which is consistent with literature reports.[29,30] The PPy and SZIF-67@PPy composite show the amorphous nature and all of the peaks of SZIF-67 vanished in SZIF-67@PPy.[22] It is due to the excessive coating of amorphous PPy on the surface of SZIF-67.[31,32] Electron paramagnetic resonance spectroscopy (EPR) is employed to analyze the presence of free electrons, as EPR is a sensitive technique to analyze electronic contributions in a material (Fig. 2b). The g-factor was calculated by Eq.1:

$$g = \frac{h\nu}{\mu_B B} \quad (1)$$

here h is the Planck's constant, ν is the applied microwave frequency (9.878 GHz), μ_B is the Bohr magneton, and B is the applied resonance magnetic field.[33] The g factor has been calculated for SZIF-67, PPy and SZIF-67@PPy composite as shown in Fig. 2(b). All the three curves, having a strong and symmetrical signal, with g value of 2.0019, 2.0014 and 2.0022 for SZIF-67, PPy and SZIF-67@PPy composite. The g value of SZIF-67@PPy composite is very close to the motion of free electrons (2.0023).[34,35] .

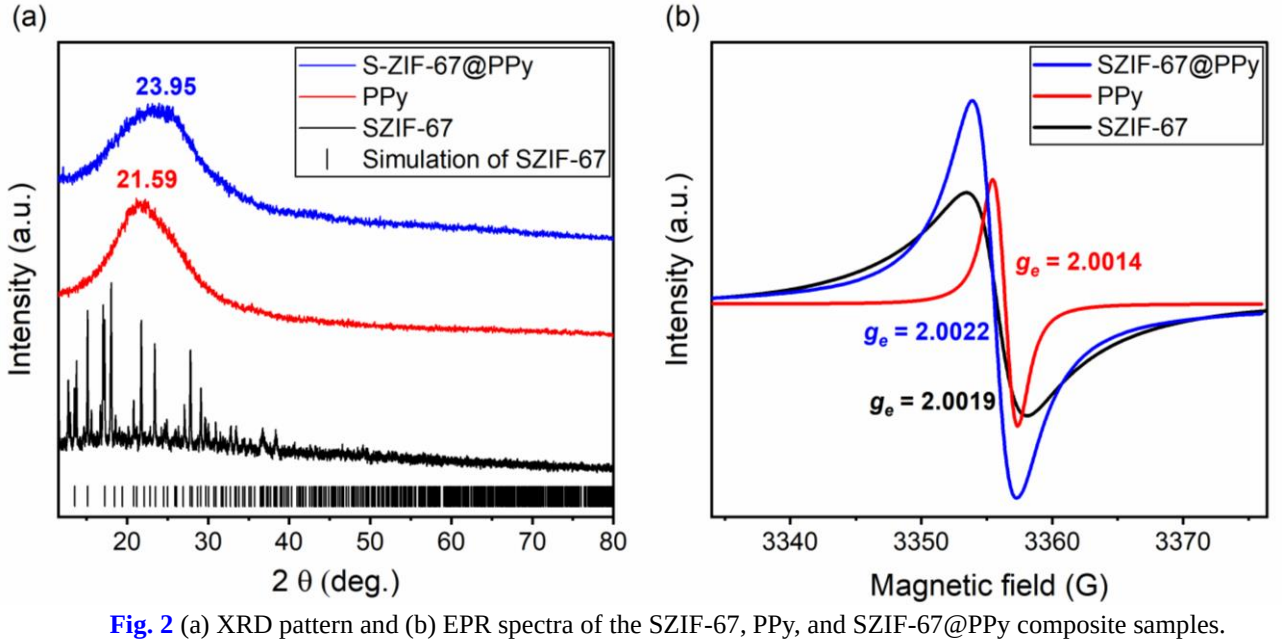

Fig. 2 (a) XRD pattern and (b) EPR spectra of the SZIF-67, PPy, and SZIF-67@PPy composite samples.

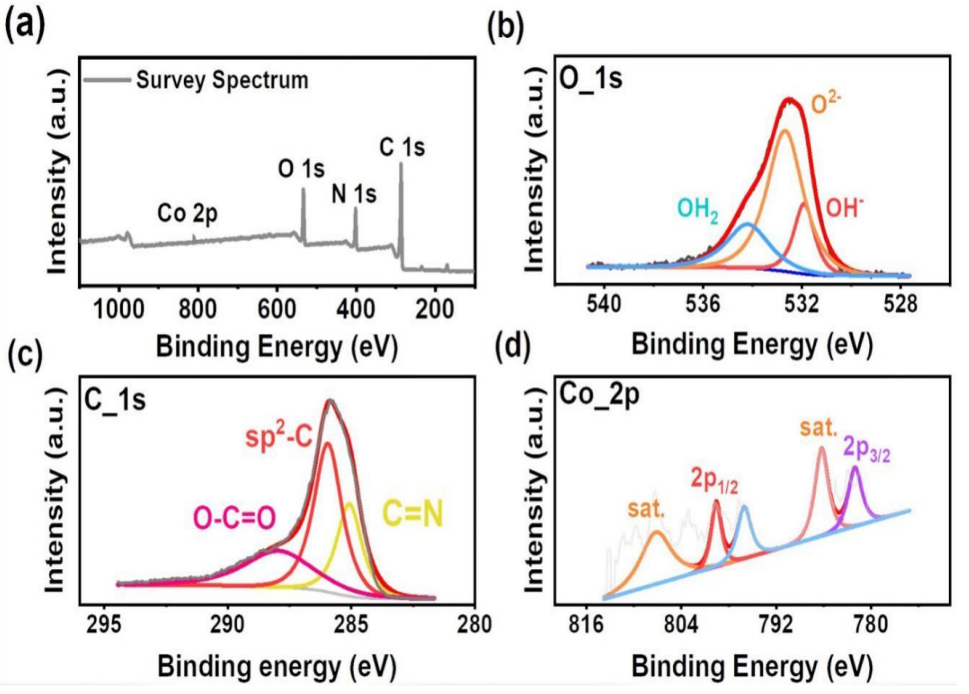

Fig. 3 XPS spectra of high-resolution (a) survey spectrum, (b) C 1s Spectrum, (c) O 1s spectrum and (d) Co 2p spectrum of SZIF-67@PPy composite.

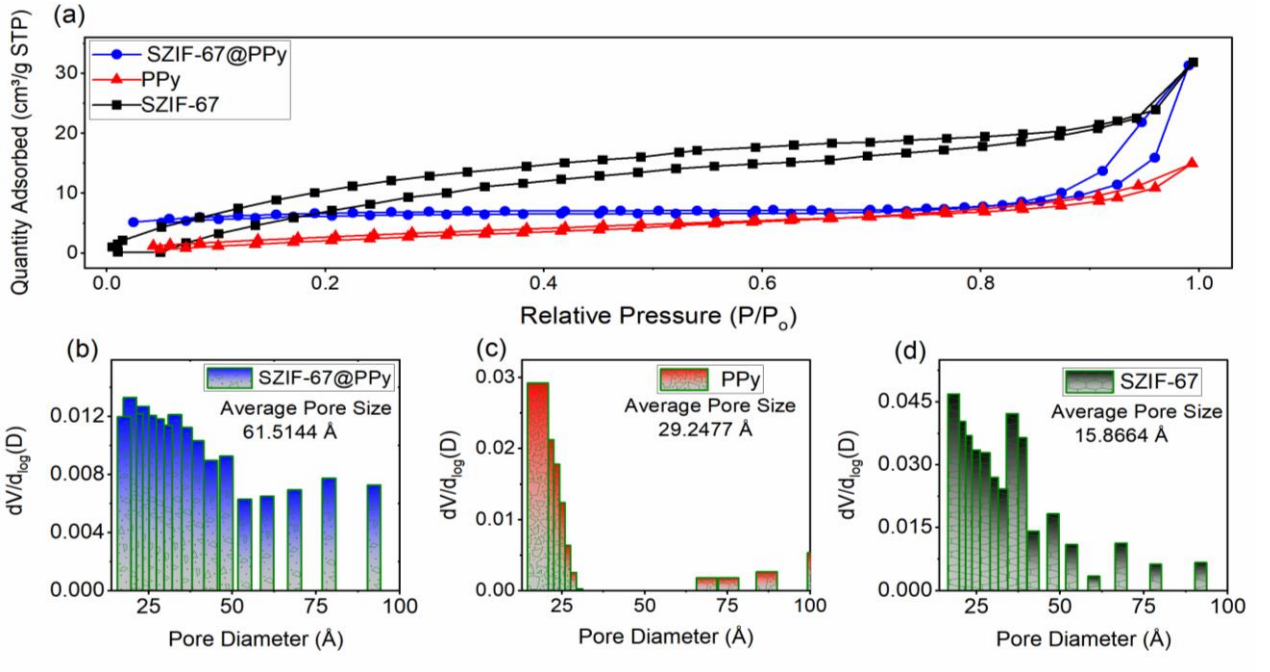

Fig. 4 (a) N_2 adsorption-desorption isotherms and pore diameter of (b) SZIF-67@PPy, (c) PPy and (d) SZIF-67@PPy composite via BJH adsorption, respectively.

Moreover, in a normalized intensity unit (free electrons number per mole), the EPR signal intensity of SZIF-67@PPy composite is much stronger than SZIF-67 and PPy. This enhanced EPR signal originates from the increased amount of O^+ centers. These O-vacancies are the donor defects that can yield electrons that can lead to the electron hopping between Co^{2+} and Co^{3+} ions giving rise to electronic conductivity.

Fig. 3 shows the XPS survey spectrum, C 1s Spectrum, O 1s spectrum and Co 2p spectrum of SZIF-67@PPy composite. The XPS survey spectrum as shown in Fig. 3(a) confirms the presence of carbon, oxygen, nitrogen and cobalt. The high-resolution O 1s spectrum (shown in Fig. 3(b)) is deconvoluted into three peaks, where peak I belongs to the carbonyl oxygen of quinines, peak II corresponds to the oxygen of hydroxyl groups and the peak III corresponds to the absorbed water or humidity.[34,36–38] Fig. 3(c) shows the C 1s XPS energy spectrum, where the peak at 285.96 eV corresponds to the benzene structure on the main chain of polypyrrole, the peak at

284.45 eV represents the C of sp^2 hybrid orbit on the main chain of PPy, and the peak at 284.81 eV corresponds to the quinone structure (q) of the main chain of PPy.[39] The XPS spectrum of Co metal shown in Fig. 3(d) contains two characteristic peaks corresponding to Co $2p_{3/2}$ and Co $2p_{1/2}$ at 781.1 eV and 796.7 eV, as well as two shake-up satellite peaks, respectively.[40–42]

The Brunauer–Emmett–Teller (BET) surface areas and pore diameter distribution of SZIF-67, PPy and SZIF-67@PPy composite were measured through N_2 adsorption-desorption isotherms (Fig. 4). The surface area of SZIF-67@PPy composite is 32.05 $m^2 g^{-1}$ which is slightly increased compared with SZIF-67 (27.18 $m^2 g^{-1}$) and PPy (11.28 $m^2 g^{-1}$). Moreover, the pore diameter distribution curves show large variance. The enhanced pores in the composite showing more tendency for N_2 adsorption and desorption. These pores in SZIF-67@PPy composite suggests that the nanocomposite have more active sites for the ion channeling and ion conductivity.

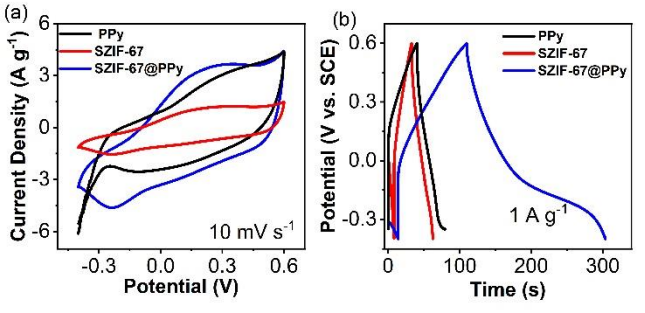

Fig. 5 Electrochemical measurements: (a) CV at 10 mVs-1 and (b) GCD curves at 1 Ag^{-1} of PPy, SZIF-67, and SZIF-67@PPy composite, respectively.

Generally, the electrochemical properties of electrode materials for supercapacitors can be studied by using three-electrode or two electrode systems. However, the capacitance measured in the three-electrode system is usually better than the two electrode system.[43] Fig. 5 shows the CV curves at 10 mVs-1 (a) and GCD curves at 1 Ag^{-1} (b) of SZIF-67, PPy, and SZIF-67@PPy composite in the three-electrode system. Generally, the C-V curve of an ideal double-layer capacitor is similar to a parallelogram, but the internal resistance of the electrode material will cause the loss of the cyclic voltammetric curve of the double-layer capacitor.[44,45] For PPy, which is a pseudocapacitor electrode material, it not only has the charge storage capacity of double-layer capacitor but also has the redox charge storage capacity.[46] Therefore, we can observe the redox curve on its cyclic voltammetry curve. It can be seen from Fig. 5 that the pseudocapacitance characteristic of SZIF-67@PPy is significantly stronger than that of the other two samples, which can be seen from the peak area and peak shape enclosed by cyclic voltammetry.[12,27,47] The GCD curves (as shown in Fig. 5(b) under the current density of 1 Ag^{-1}, the specific capacitance (220 F g^{-1}) of SZIF-67@PPy is much higher than that of SZIF-67(30.3 F g^{-1}) and PPy (38.7 F g^{-1}).

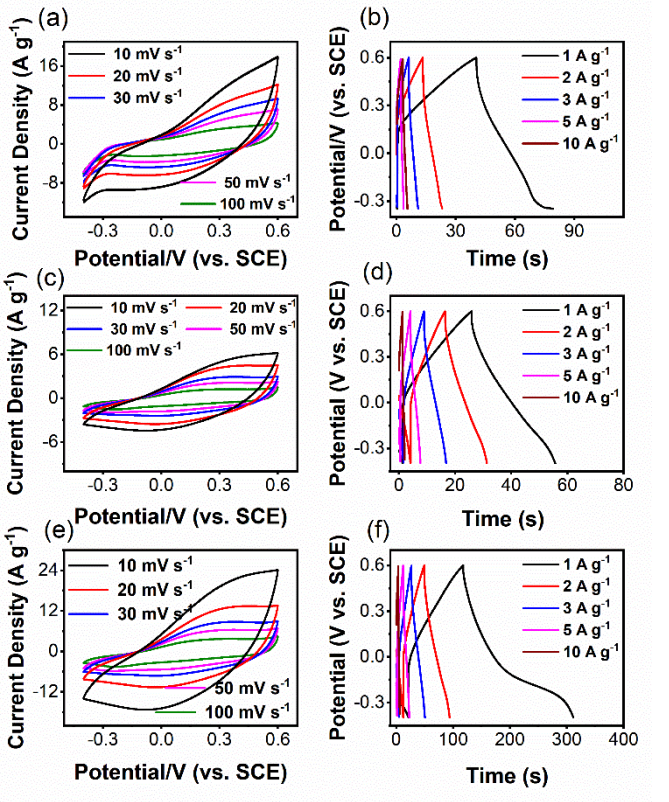

Fig. 6 Electrochemical measurements: (a, c, e) CV at different scan rates and (b, d, f) GCD curves at different current densities of PPy, SZIF-67, and SZIF-67@PPy composite, respectively.

Fig. 6 shows the cyclic voltammetry curves of (a) PPy, (c) SZIF-67 and (e) SZIF-67@PPy composite at the scan rate of 5, 10, 20, 50, 100 mVs^{-1}. It can be seen that SZIF-67@PPy keeps a good peak shape with the increase of sweep speed of applied voltage from 5 mVs^{-1} to 100 mVs^{-1}, and the parallelogram peak shape with clear redox peaks of CV is more obvious in the low sweep speed mode, which shows that it has the charge enrichment storage capacity of double-layer capacitor and the redox charge storage capacity of pseudocapacitor.[44,48–50]

As shown in Fig. 6(b, d and e) the GCD curves of PPy, SZIF-67, and SZIF-67@PPy composite samples were measured in a three-electrode system with 1 M H_2SO_4 solution as the electrolyte. The specific capacitance (C_S) of active material to a single electrode can be calculated by the following formula[51]:

$$C_s = \frac{I \times \Delta t}{m \times \Delta V} \quad (2)$$

where, Δ T, m and Δ V denote the current discharge time, the mass of the active material of the electrode and the potential window, respectively. According to Eq. (2), the specific capacitance of PPy, SZIF-67, and SZIF-67@PPy composite are 38.7, 30.3 and 220 Fg^{-1} respectively at the current density of 1 A g^{-1}. Compared with ordinary PPy and SZIF-67, the specific capacitance of SZIF-67@PPy is significantly enhanced. According to the experimental data, we infer that this is due to the increase of surface area, pores, and molecular arrangement order. On one hand, it is conducive to the

adsorption of charge, while on the other hand, it effectively reduces the internal resistance of the electrode system, thus increasing its specific capacitance. The SZIF-67@PPy nanocomposite electrode material, with SZIF-67, as an effective porous material, greatly improves the ionic charge transfer efficiency in PPy.

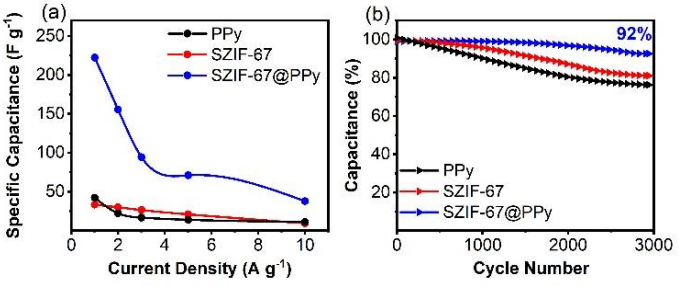

Fig. 7 (a) The specific capacitance at different current densities and (b) cycling performance at a current density of 10 A g^{-1} for PPy, SZIF-67, and SZIF-67@PPy composite, respectively.

In addition, when the current density is 1, 2, 3, 5 and 10 Ag^{-1}, the specific capacitance of SZIF-67@PPy nanocomposite electrode material is 220, 154.9, 96.1, 70.2 and 39 Fg^{-1}, respectively. Moreover, Table S1 in the supporting information enlisted the performance of MOF and PPy synthesized materials compared with this work. It can be seen that SZIF-67@PPy composite have a decent supercapacitance performance even at a very lower loading ratio. It can be seen from Fig. 7(a) that the increase of current density, SZIF-67@PPy nanocomposite electrode materials show low specific capacitance, which means that the rapid charge-discharge directly reduces the adsorption efficiency of the charge in the electrolyte on the electrode.[52] Moreover, the cycling performance of the electrode material of the supercapacitor is an important index to measure the stability of the charge-discharge performance of the electrode material. As shown in Fig. 7(b), the PPy, SZIF-67, and SZIF-67@PPy composite materials were charged and discharged for 3000 cycles at the current density of 10 A g^{-1} to evaluate the cycle stability. After 1000 charge-discharge cycles, the capacity retention of PPy (89.73%) is slightly lower than SZIF-67 (95.39%). Compared with PPy (75.82%) and SZIF-67 (81%) after 3000 cycles, the stability of SZIF-67@PPy composite was significantly sustained to 92%. Due to the high mechanical strength and excellent electrochemical stability of SZIF-67@PPy composite, it acts as an elastic framework to prevent the expansion and contraction of PPy in the repeated charge-discharge process.[53,54]

4. Conclusion

Composite of polypyrrole with SZIF-67 was prepared by in-situ oxidation polymerization with CSA as the doping acid. SZIF-67@PPy with excellent electrochemical properties were used to prepare electrode materials for supercapacitors. The electrode has larger specific capacitance and good capacity retention after 3000 cycles. Compared with conductive PPy and SZIF-67, the composite of SZIF-67@PPy effectively improves the charge transfer capacity of conductive polymer, reduces the internal resistance of the system, effectively improves the specific capacitance and cycle stability. The results indicate that SZIF-67@PPy can be a good candidate for high performance, flexible and stable electrode material of supercapacitor.

Acknowledgment

The authors are highly thankful to the National Natural Science Foundations of China for their financial support (Grant No. 3190110313 to Kun Ma, U1632274 to Junfeng Wang), and Ministry of Science and Technology of China (2016YFA0400901 to Junfeng Wang). A portion of this work was performed on the Steady High Magnetic Field Facilities, High Magnetic Field Laboratory, CAS.

Supporting information

Not applicable

Conflict of interest

There are no conflicts to declare.

Reference

[1] N. L. Torad, R. R. Salunkhe, Y. Li, H. Hamoudi, M. Imura, Y. Sakka, C. Hu and Y. Yamauchi, *Chem. Eur. J.*, 2014, **20**, 7895–7900, doi: 10.1002/chem.201400089.

[2] S. S. Patil, T. S. Bhat, A. M. Teli, S. A. Beknalkar, S. B. Dhavale, M. M. Faras, M. M. Karanjkar and P. S. Patil, *Eng. Sci.*, 2020, **12**, 38–51, doi: 10.30919/es8d1140.

[3] T. Chen and L. Dai, *J. Mater. Chem. A*, 2014, **2**, 10756, doi: 10.1039/C4TA00567H.

[4] R. Nie, Q. Wang, P. Sun, R. Wang, Q. Yuan and X. Wang, *Eng. Sci.*, 2019, **6**, 22–29, doi: 10.30919/es8d668.

[5] K. M. Popov, V. E. Arkhipov, A. G. Kurenya, E. O. Fedorovskaya, K. A. Kovalenko, A. V Okotrub and L. G. Bulusheva, *Phys. status solidi*, 2016, **253**, 2406–2412, doi: 10.1002/pssb.201600240.

[6] S. G. Sayyed, M. A. Mahadik, A. V Shaikh, J. S. Jang and H. M. Pathan, *ES Energy Environ.*, 2019, **3**, 25–44, doi: 10.30919/esee8c211.

[7] I. Shown, A. Ganguly, L. Chen and K. Chen, *Energy Sci. Eng.*, 2015, **3**, 2–26, doi: 10.1002/ese3.50.

[8] X. Li, W. Zhao, R. Yin, X. Huang and L. Qian, *Eng. Sci.*, 2018, **3**, 89–95, doi: 10.30919/es8d743.

[9] H. Huang, L. Han, Y. Wang, Z. Yang, F. Zhu and M. Xu, *Eng. Sci.*, 2019, **9**, 60–67, doi: 10.30919/es8d812.

[10] H. Kashani, L. Chen, Y. Ito, J. Han, A. Hirata and M. Chen, *Nano Energy*, 2016, **19**, 391–400, doi: 10.1016/j.nanoen.2015.11.029.

[11] A. Lamberti, A. Gigot, S. Bianco, M. Fontana, M. Castellino, E. Tresso and C. F. Pirri, *Carbon*, 2016, **105**, 649–654, doi: 10.1016/j.carbon.2016.05.003.

[12] J. Xu, D. Wang, Y. Yuan, W. Wei, L. Duan, L. Wang, H. Bao and W. Xu, *Org. Electron. physics, Mater. Appl.*, 2015, **24**, 153–159, doi: 10.1016/j.orgel.2015.05.037.

[13] V. Elayappan, V. Murugadoss, Z. Fei, P. J. Dyson and S. Angaiah, 2020, **10**, 78–84, doi: 10.30919/es5e1007.

[14] S. Farid, W. Qiu, J. Zhao, X. Song, Q. Mao, S. Ren and C. Hao, *J. Electroanal. Chem.*, 2019, **858**, 113768, doi: 10.1016/j.jelechem.2019.113768.
[15] J. Guo, H. Song, H. Liu, C. Luo, Y. Ren, T. Ding, M. A. Khan, D. P. Young, X. Liu, X. Zhang, J. Kong and Z. Guo, *J. Mater. Chem. C*, 2017, **5**, 5334–5344, doi: 10.1039/C7TC01502J.
[16] R. McNeill, R. Siudak, J. H. Wardlaw and D. E. Weiss, *Aust. J. Chem.*, 1963, **16**, 1056–1075, doi: 10.1071/CH9631056.
[17] A. G. MacDiarmid, *Angew. Chemie Int. Ed.*, 2001, **40**, 2581–2590, doi: 10.1002/1521-3773(20010716)40:14<2581::AID-ANIE2581>3.0.CO;2-2.
[18] R. Hou, M. Miao, Q. Wang, T. Yue, H. Liu, H. S. Park, K. Qi and B. Y. Xia, *Adv. Energy Mater.*, 2019, 1901892, doi: 10.1002/aenm.201901892.
[19] J. Liu, Z. Wang, S. ur Rehman and H. Bi, *RSC Adv.*, 2017, **7**, 53104–53110, doi: 10.1039/C7RA08132D.
[20] Y. Wang, Y. Liu, C. Wang, H. Liu, J. Zhang, J. Lin, J. Fan, T. Ding, J. E. Ryu and Z. Guo, *Eng. Sci.*, 2020, **9**, 50–59, doi: 10.30919/es8d903.
[21] Q. Jiang, Z. Guo, G. Yang, E. Wujick and H. Gu, *Eng. Sci.*, 2020, **9**, 1–2, doi: 10.30919/es8d916.
[22] J. Liu, S. ur Rehman, J. Wang, Z. Fang, X. Zhang and H. Bi, *Synth. Met.*, 2018, **246**, 23–30, doi: 10.1016/j.synthmet.2018.09.015.
[23] S. ur Rehman, J. Liu, Z. Fang, J. Wang, R. Ahmed, C. Wang and H. Bi, *ACS Appl. Nano Mater.*, 2019, **2**, 4451–4461, doi: 10.1021/acsanm.9b00841.
[24] X. Liang, B. Quan, Z. Man, B. Cao, N. Li, C. Wang, G. Ji and T. Yu, *ACS Appl. Mater. Interfaces*, 2019, **11**, 30228–30233, doi: 10.1021/acsami.9b08365.
[25] W. Gu, J. Tan, J. Chen, Z. Zhang, Y. Zhao, J. Yu and G. Ji, *ACS Appl. Mater. Interfaces*, 2020, **12**, 28727-28737, doi: 10.1021/acsami.9b19768.
[26] X. Liang, Z. Man, B. Quan, J. Zheng, W. Gu, Z. Zhang and G. Ji, *Nano-Micro Lett.*, 2020, **12**, 102, doi: 10.1007/s40820-020-00432-2.
[27] X. Xu, J. Tang, H. Qian, S. Hou, Y. Bando, M. S. A. Hossain, L. Pan and Y. Yamauchi, *ACS Appl. Mater. Interfaces*, 2017, **9**, 38737–38744, doi: 10.1021/acsami.7b09944.
[28] H. Dong, Y. Li, H. Chai, Y. Cao and X. Chen, *ES Energy Environ.*, 2019, **4**, 19–26, doi: 10.30919/esee8c221.
[29] K. Zhou, B. Mousavi, Z. Luo, S. Phatanasri, S. Chaemchuen and F. Verpoort, *J. Mater. Chem. A*, 2017, **5**, 952–957, doi: 10.1039/C6TA07860E.
[30] X. Zhang, G. Ji, W. Liu, B. Quan, X. Liang, C. Shang, Y. Cheng and Y. Du, *Nanoscale*, 2015, **7**, 12932–12942, doi: 10.1039/C5NR03176A.
[31] J. Liu, S. ur Rehman, Z. Fu, Y. Liu, Y. Lu, H. Bi and P. C. Morais, *Synth. Met.*, 2019, **253**, 131–140, doi: 10.1016/j.synthmet.2019.05.009.
[32] S. ur Rehman, M. Sun, M. Xu, J. Liu, R. Ahmed, M. Adnan Aslam, R. Ali Ahmad and H. Bi, *J. Colloid Interface Sci.*, 2020, **574**, 87–96, doi: 10.1016/j.jcis.2020.04.053.
[33] Y. Xia, Y. Li, A. O. Burts, M. F. Ottaviani, D. A. Tirrell, J. A. Johnson, N. J. Turro and R. H. Grubbs, *J. Amer. Chem. Soc.*, 2011, **133**, 19953–19959, doi: 10.1021/ja2085349.
[34] R. Ahmed, J. Wang, R. J. Si, S. ur Rehman, T. Li, H. Bi, Y. Yu, Q. J. Li, Y. D. Li and S. G. Huang, *J. Eur. Ceram. Soc.*, doi: 10.1016/j.jeurceramsoc.2020.11.034.
[35] Z. Fang, S. ur Rehman, M. Sun, Y. Yuan, S. Jin and H. Bi, *J. Mater. Chem. A*, 2018, **6**, 21131–21142, doi: 10.1039/C8TA08262F.
[36] J. H. Zhou, Z. J. Sui, J. Zhu, P. Li, D. Chen, Y. C. Dai and W. K. Yuan, *Carbon,* 2007, **45**, 785–796, doi: 10.1016/j.carbon.2006.11.019.
[37] R. Ahmed, S. ur Rehman, R. Si and C. Wang, *Phys. Status Solidi Basic Res.*, 2020, 2000342.
[38] R. Ahmed, R. Si, S. ur Rehman, Y. Yu, Q. Li and C. Wang, *Results Phys.*, 2020, 103623, doi: 10.1016/j.rinp.2020.103623.
[39] J. Tabačiarová, M. Mičušík, P. Fedorko and M. Omastová, *Polym. Degrad. Stab.*, 2015, **120**, 392-401, doi: 10.1016/j.polymdegradstab.2015.07.021.
[40] S. ur Rehman, R. Ahmed, J. Liu, J. Wang, M. Sun, Z. Fang, M. A. Aslam, P. C. Morais, C. Wang and H. Bi, *Part. Part. Syst. Charact.*, 2019, **36**, 1900047, doi: 10.1002/ppsc.201900047.
[41] S. ur Rehman, J. Wang, Q. Luo, M. Sun, L. Jiang, Q. Han, J. Liu and H. Bi, *Chem. Eng. J.*, 2019, **373**, 122–130, doi: 10.1016/j.cej.2019.05.040.
[42] W. Uddin, S. ur Rehman, M. A. Aslam, S. ur Rehman, M. Wu and M. Zhu, *Mater. Res. Bull.*, 2020, **130**, 110943, doi: 10.1016/j.materresbull.2020.110943.
[43] J. Y. Song, H. H. Lee, Y. Y. Wang and C. C. Wan, *J. Power Sources*, 2002, **111**, 255–267, doi: 10.1016/S0378-7753(02)00310-5.
[44] D. Sheberla, J. C. Bachman, J. S. Elias, C. J. Sun, Y. Shao-Horn and M. Dincă, *Nat. Mater.*, 2017, **16**, 220–224, doi: 10.1038/nmat4766.
[45] K. K. Denshchikov, M. Y. Izmaylova, A. Z. Zhuk, Y. S. Vygodskii, V. T. Novikov and A. F. Gerasimov, *Electrochim. Acta*, 2010, **55**, 7506–7510, doi: 10.1016/j.electacta.2010.03.065.
[46] J. Wang, Y. Xu, X. Chen and X. Du, *J. Power Sources*, 2007, **163**, 1120–1125, doi: 10.1016/j.jpowsour.2006.10.004.
[47] M.-X. Wang, J. Zhang, H.-L. Fan, B.-X. Liu, X.-B. Yi and J.-Q. Wang, *New J. Chem.*, 2019, **43**, 5666–5669, doi: 10.1039/C8NJ05958F.
[48] D. Vonlanthen, P. Lazarev, K. A. See, F. Wudl and A. J. Heeger, *Adv. Mater.*, 2014, **26**, 5095–5100, doi: 10.1002/adma.201400966.
[49] G. A. Snook, P. Kao and A. S. Best, *J. Power Sources*, 2011, **196**, 1–12, doi: 10.1016/j.jpowsour.2010.06.084.
[50] W. Chen, R. B. Rakhi and H. N. Alshareef, *Nanoscale*, 2013, **5**, 4134, doi: 10.1039/C3NR00773A.
[51] P. Cai, T. Liu, L. Zhang, B. Cheng and J. Yu, *Appl. Surf. Sci.*, 2020, **504**, 144501, doi: 10.1016/j.apsusc.2019.144501.
[52] A. Eftekhari, L. Li and Y. Yang, *J. Power Sources*, 2017, **347**, 86–107, doi: 10.1016/j.jpowsour.2017.02.054.
[53] C. Liu, F. Li, L.-P. Ma and H.-M. Cheng, *Adv. Mater.*, 2010, **22**, E28–E62, doi: 10.1002/adma.200903328.

[54] K. S. Ryu, K. M. Kim, N. G. Park, Y. J. Park and S. H. Chang, *J. Power Sources*, 2002, **103**, 305–309, doi: 10.1016/S0378-7753(01)00862-X.

Author information

Sajid ur Rehman *received his PhD degree in Polymer Chemistry and Physics from Anhui University, Hefei, China. Currently, he is on Post doctoral position at High Magnetic Field Laboratory, Hefei Institute of Physical Sciences, Chinese Academy of Sciences, Hefei, China. His research focus is on biomaterials, energy storage devices and microwave absorption properties.*

Rida Ahmed *received her Ph.D degree in Materials Physics from Anhui University, Hefei, P. R. China. Her research is focused on dielectric materials and energy storage devices.*

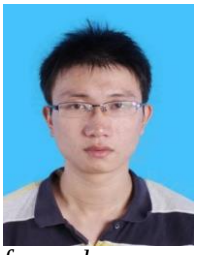

Kun Ma *received PhD degree in Biophysics from University of Chinese Academy of Sciences. He is currently at Researcher Associate position at High Magnetic Field Laboratory, Hefei Institute of Physical Sciences, Chinese Academy of Sciences, Hefei, China. His research is focused on nanomaterials for biomedical and energy-related applications.*

Shuai Xu *received his B.S. degree in biotechnology from Anhui University in 2013 and is currently a PhD candidate in biophysics from University of Science and Technology of China. He is now studying in High Magnetic Field Laboratory, CAS, working with biomimetic nanoparticles for biomedical and energy-related applications.*

Tongxiang Tao *received his B.S. degree from Anhui Science and Technology University in 2016 and is currently a PhD student in biophysics at University of Science and Technology of China . Now he is studying at High Magnetic Field Laboratory of the Chinese Academy of Sciences.His research focus on bio-material energy storage devices and bio-inspired nanobiology.*

Muhammad Adnan Aslam *received his M.S degree in Nanotechnology from University of the Punjab, Pakistan in 2016 and a graduate student pursuing his PhD in Condensed matter physics from High magnetic field laboratory, Hefei institutes of physical science, Chinese Academy of Sciences, China. His current research includes synthesis of nanomaterials under applied magnetic field, bio-waste, industrial waste materials for microwave absorption, and energy storage devices.*

Muhammad Amir *received his MS degree in Physics from COMSATS Institute of Information Technology Lahore, in 2016, and currently a Ph.D. scholar in Dalian University of Technology, Dalian. Currently his research interest is Laser Induced Breakdown Spectroscopy(LIBS), which includes Pulsed Laser Deposition(PLD), theoretically modeling and simulation of different materials.*

Dr. Junfeng Wang, *Professor, deputy director of the Hefei institute of Physical Sciences, CAS, China, and director of the magnetic resonance and life science division.He received his PhD degree from National High Magnetic Field Laboratory/Florida State University in 2001. Before joining CHMFL as a "Hundred Talents Program" researcher of Chinese Academy of Sciences, he conducted postdoctoral researches at University of Georgia and Harvard Medical School.The ongoing researches in his lab focus on membrane protein structure determination, protein-lipid interactions and biomaterials applications.*

